Abnormal transport along the lysosomal pathway in Mucolipidosis, type IV disease

Chii-Shiarng Chen*, Gideon Bach[†], and Richard E. Pagano*[‡]

*Department of Biochemistry and Molecular Biology, Thoracic Diseases Research Unit, Mayo Clinic and Foundation, 200 First Street S.W., Rochester, MN 55905-0001; and †Department of Human Genetics, Hadassah University Hospital, Jerusalem, Israel

ABSTRACT Mucolipidosis, type IV (ML-IV) is an autosomal recessive storage disease that is characterized by lysosomal accumulation of sphingolipids, phospholipids, and acid mucopolysaccharides. Unlike most other storage diseases, the lysosomal hydrolases participating in the catabolism of the stored molecules appear to be normal. In the present study, we examined the hypothesis that the ML-IV phenotype might arise from abnormal transport along the lysosomal pathway. By using various markers for endocytosis, we found that plasma membrane internalization and recycling were nearly identical in ML-IV and normal fibroblasts. A fluorescent analog of lactosylceramide (LacCer) was used to study plasma membrane lipid internalization and subsequent transport. Lipid internalization at 19°C was similar in both cell types; however, 40–60 min after raising the temperature to 37°C, the fluorescent lipid accumulated in the lysosomes of ML-IV cells but was mainly concentrated at the Golgi complex of normal fibroblasts. Biochemical studies demonstrated that at these time points, hydrolysis of the lipid analog was minimal ($\sim$7%) in both cell types. A fluorescence ratio imaging assay was developed to monitor accumulation of fluorescent LacCer in the lysosomes and showed that the apparent concentration of the lipid increased more rapidly and to a greater extent in ML-IV cells than in normal fibroblasts. By 60 min, LacCer apparently decreased in the lysosomes of normal fibroblasts but not in ML-IV cells, suggesting that lipid efflux from the lysosomes was also impaired. These results demonstrate that there is a defect in ML-IV fibroblasts that affects membrane sorting and/or late steps of endocytosis.

Mucolipidosis, type IV (ML-IV) is an autosomal recessive lysosomal storage disease that is characterized clinically by psychomotor retardation and ophthalmological abnormalities including cornea opacity, retinal degeneration, and strabismus (for reviews, see refs. 1–3). Most of the patients diagnosed with ML-IV disease are Ashkenazi Jews living either in the United States or Israel and range from 1 to approximately 40 years of age. The prognosis beyond this age, and the life expectancy of these patients is not known. Electron microscopy investigations have demonstrated lysosomal storage of lipids and water-soluble substances in cells from every tissue or organ of ML-IV patients. This heterogeneous storage characterizes the disease as a mucolipidosis. The storage materials have been identified as sphingolipids, phospholipids, and acid mucopolysaccharides. The metabolic defect causing this accumulation has not yet been identified nor has the relevant gene been mapped or cloned. Unlike most other lipid storage diseases in which lysosomal hydrolases or activator proteins are defective, extensive studies have shown normal activities of all the lysoso-

mal hydrolases participating in the catabolism of the stored macromolecules in ML-IV cells (3), suggesting an alternative mechanism for storage in this cell type. Preliminary studies using exogenous radioactive phosphatidylcholine, one of the major lipid classes that accumulates in ML-IV, showed increased retention in the lysosomes of ML-IV fibroblasts but normal degradation (4), suggesting an abnormality in endocytosis rather than degradation as a cause for this storage. In the present study, we examined the movement of various markers along the lysosomal pathway and document a substantial alteration in the kinetics of intracellular transport in ML-IV cells.

MATERIALS AND METHODS

Cells and Cell Culture. ML-IV cells were obtained from skin biopsies of patients diagnosed with this disease at Hadassah University Hospital. Normal human skin fibroblasts (GM 5659C) and fibroblasts from patients with Hunter (GM 298) and Pompe disease (GM 1935) were obtained from the Coriell Institute, Human Genetic Mutant Cell Repository (Camden, NJ). Fibroblasts from patients with Hurler syndrome were obtained from the Department of Laboratory Medicine and Pathology of the Mayo Clinic. Cells were cultured as described (1, 5). All experiments were performed on monolayer cultures grown to 30–50% confluency on acid-etched glass coverslips for microscopy (6) or on 60- or 100-mm diameter tissue culture dishes for biochemical experiments.

Incubation of Cells with a Fluorescent Analog of Lactosylceramide (LacCer) and Fluorescent Dextran. In double-label experiments, cell cultures were incubated with Cascade blue-conjugated dextran (10 kDa, lysine fixable; Molecular Probes) at 4 mg/ml in culture medium for 48 hr at 37°C before incubation with fluorescent lipid. Under these conditions, almost all of the internalized dextran was found in lysosomes as shown with another fluorescent dextran (5).

A fluorescent analog of lactosylceramide, *N*-[5-(5,7-dimethyl BODIPY)-1-pentanoyl]-lactosyl sphingosine (C_5-DMB-LacCer), where BODIPY is boron dipyrromethene difluoride, was synthesized and purified as described (6). A BSA complex of the fluorescent lipid (7) was then prepared in HMEM [10 mM 4-(2-hydroxyethyl)-1-piperazineethanesulfonic acid-buffered MEM (pH 7.4) without indicator] and stored at −20°C. Cells were incubated with 5 μM C_5-DMB-LacCer/BSA at 19°C or 37°C, washed with ice-cold HMEM, back-

---

exchanged with 5% BSA to remove fluorescent lipid present at the plasma membrane (6, 8), and further incubated at 37°C for various times.

Fluorescence Microscopy. Fluorescence microscopy was performed as described (9). Details of quantitative microscopy and image processing are given elsewhere (8). For Cascade blue, samples were excited at 365 nm and fluorescence observed at ≥420 nm. For BODIPY fluorescence, samples were excited at 450–490 nm and viewed at "green" (520–560 nm), "green + red" ($\lambda_{em} \geq 520$ nm) or "red" ($\lambda_{em} \geq 590$ nm) wavelengths.

Biochemical Analyses. Cells were incubated with C_5-DMB-LacCer under various conditions and back-exchanged. The cells were then washed, scraped from the culture dish, and centrifuged, and the fluorescent lipids were extracted (10). Fluorescent lipids were analyzed by TLC using C/MeOH/15 mM $CaCl_2$, 60:35:8 (vol/vol), as the developing solvent. TLC plates were photographed under UV light; individual spots were identified by comparison with known fluorescent standards and quantified by image analysis (11). Endogenous cellular lipids were extracted, saponified, and desalted as described (12). In some cases, cells were incubated with 1 μCi/ml [1-^{14}C] palmitate (Amersham) for 4 days before lipid extraction. Lipid extracts, corresponding to equal amounts of cellular protein, were then separated by TLC using C/MeOH/15 mM $CaCl_2$ or C/MeOH, 9:1 (vol/vol), as the developing solvent, and visualized with anisaldehyde/sulfuric acid (13) or by autoradiography. For experiments with [1-^{14}C]palmitate, lipid extracts of cells from two ML-IV patients were used (five determinations). Radioactivity was quantified by using a phosphoimager (Molecular Analyst GS-363, Bio-Rad). Endogenous ceramide was identified by using natural ceramide samples as standards.

Internalization of Various Markers at 19°C. For fluid phase uptake, cells were incubated with horseradish peroxidase (HRP) at 2 mg/ml in HMEM/10% fetal bovine serum for 60 min at 19°C, and the uptake of HRP was quantified (14, 15) and normalized to total cellular protein (16). For plasma membrane lipid uptake, cells were incubated with C_5-DMB-LacCer for 60 min at 19°C and washed. Any fluorescent lipid present at the plasma membrane was then removed by back-exchange (6, 8). The amount of internalized C_5-DMB-LacCer was then quantified by extraction and analysis of the cell-associated fluorescent lipid that remained after these procedures. For receptor mediated endocytosis, human transferrin (Tfn) was radiolabeled with ^{125}I and chloramine T and purified as described (17). Cells were incubated with iodinated transferrin (^{125}I-Tfn) for 60 min at 19°C and washed. The cells were then chilled to 4°C and briefly treated with acid saline to "strip" any ^{125}I-Tfn from the cell surface (18), and the uptake quantified by γ counting. Data were normalized to cellular protein (16). (In control experiments, ≥99% of the ^{125}I-Tfn bound at 4°C could be displaced with a 100-fold excess of unlabeled Tfn.)

Transport from Endosomes to the Plasma Membrane. Cells were incubated with ^{125}I-Tfn for 60 min at 19°C as above. After acid stripping, the cells were warmed to 37°C for various times. At each time point, the amount of ^{125}I-Tfn released into the medium (and remaining in the cells) was quantified and normalized to cellular DNA (19) to provide a measure of the recycling of the Tfn receptor.

Lipid Transport from Endosomes to Lysosomes. Cells were incubated 48 hr with fluorescent blue dextran to prelabel the lysosomes (see above). The cells were then washed, incubated with C_5-DMB-LacCer at 19°C to label the sorting endosomes, and back-exchanged to remove plasma membrane fluorescence. The cultures were then warmed to 37°C for various times (to allow transport to the lysosomes to occur), chilled to 4°C, and observed under the fluorescence microscope at 4°C using a temperature controlled stage.

For data analysis, three low-light-level images of a given cell were acquired to observe blue dextran, and the "green" and "red" components of BODIPY fluorescence. [All images were corrected for background fluorescence (8); ML-IV samples were also corrected for high autofluorescence that is observed in lysosomes (20).] A threshold level was then determined so that all the lysosomes in a portion of the blue dextran image were included, and a mask (8, 21) defined by that threshold value was used to isolate the lysosomes within that region. The mask was then used to identify those regions of the "red" and "green" images that corresponded to lysosomes so that the "red" and "green" intensity of each lysosome could be calculated. To minimize the possibility that fluorescence identified by the "lysosome mask" might actually come from another organelle, regions of the image were selected that contained no obvious overlap with the Golgi apparatus. (Several hundred lysosomes from a number of identically treated cells comprised the data set for each time point.) The red/green fluorescence (R/G) ratio of the lysosomes were then averaged and displayed vs. time to quantify temporal changes in the lysosomal accumulation of the fluorescent lipid.

RESULTS AND DISCUSSION

Accumulation and Degradation of C_5-DMB-LacCer in ML-IV Cells. Lipid analogs labeled with the BODIPY fluorophore exhibit a concentration-dependent spectral shift, emitting at green wavelengths when present at low concentrations in membranes and at red wavelengths when present at high concentrations (9). Thus, increases in concentration are reflected by an increase in the R/G ratio. This property can be used to examine the lysosomal accumulation of BODIPY-lipids in sphingolipid storage diseases (22). In the present study, we used C_5-DMB-LacCer, a BODIPY analog of LacCer, and examined its distribution in normal vs. ML-IV fibroblasts in pulse–chase experiments. A typical result is shown in Fig. 1. Cells were incubated overnight with blue dextran to prelabel the lysosomes (5) and then incubated with C_5-DMB-LacCer for 1 hr at 37°C. The cells were then washed and chased 1 hr at 37°C before observation under the fluorescence microscope. In ML-IV cells, a punctate pattern of BODIPY fluorescence was observed that colocalized with a subset of the blue dextran-labeled lysosomes, but in normal cells, a reticular and perinuclear pattern of BODIPY fluorescence corresponding to the Golgi apparatus (9, 23–25) was seen, with little labeling of the lysosomes (Fig. 1a). Furthermore, observations of BODIPY fluorescence in different regions of the spectrum demonstrated a shift in BODIPY fluorescence toward red wavelengths, consistent with the accumulation of C_5-DMB-LacCer (and/or its metabolites) in the lysosomes of ML-IV (but not normal) cells (Fig. 1b). The lysosomal accumulation seen in ML-IV cells was not unique to C_5-DMB-LacCer but was also observed using BODIPY-labeled sphingomyelin or GM_1 ganglioside (data not shown). Lysosomal accumulation of these lipids in ML-IV cells was also seen after a 1-hr pulse at 19°C followed by a 30–60 min chase at 37°C (see below).

The lysosomal accumulation of C_5-DMB-lipid was surprising because there are no reported defects in ML-IV cells in the enzymes (β-galactosylceramidase and GM1-β-galactosidase) or the activator proteins (sap-A, sap-B, and sap-C) that participate in the lysosomal degradation of LacCer. In agreement with this, lipid extraction and analysis of cells that were pulse-labeled with C_5-DMB-LacCer under various conditions showed that the amount of C_5-DMB-LacCer hydrolysis in ML-IV cells and normal fibroblasts were very similar (Table 1). Furthermore, when C_5-DMB-LacCer was incubated with Hunter, Hurler, or Pompe disease fibroblasts that contain enlarged lysosomes with stored materials, a pattern of fluorescence similar to that shown for normal human skin fibroblasts (see Fig. 1) was seen (data not shown), ruling out the
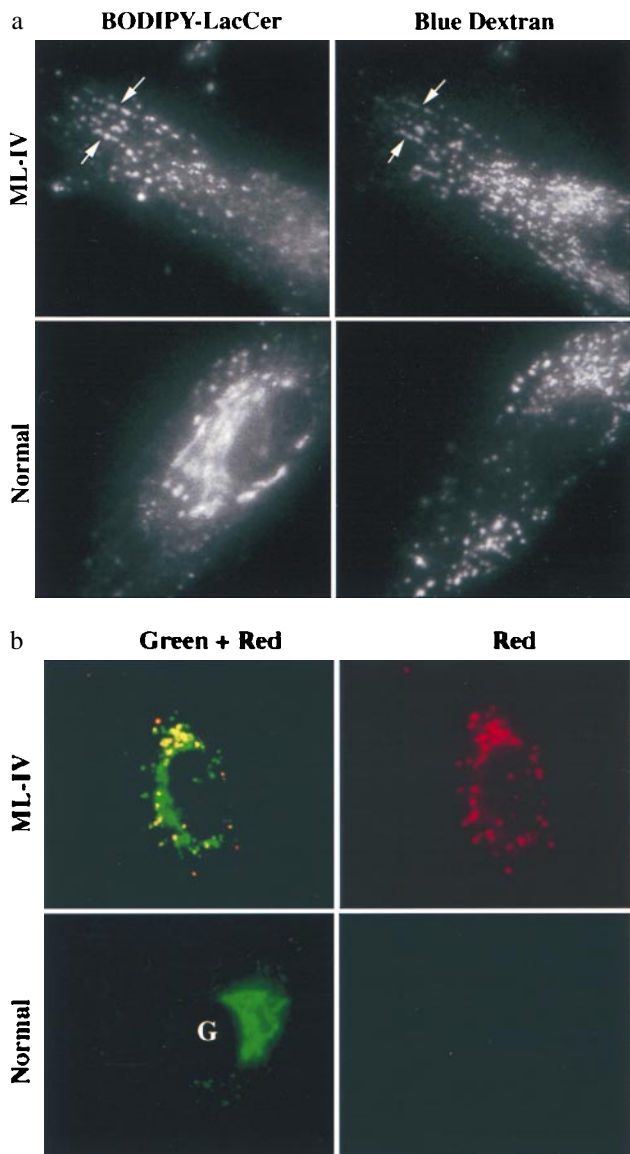
FIG. 1. Lysosomal accumulation of C$_5$-DMB-LacCer in ML-IV cells. Normal and ML-IV fibroblasts were incubated overnight with a blue fluorescent dextran to label the lysosomes and subsequently pulse-labeled with C$_5$-DMB-LacCer (see text). (*a*) In ML-IV cells, many of the punctate structures labeled with the fluorescent lipid colocalized with the dextran-stained lysosomes (e.g., at arrows), but in normal fibroblasts most of the fluorescent lipid was observed at the Golgi complex (G), with little present in the lysosomes. (*b*) Observations of BODIPY fluorescence in different regions of the spectrum also demonstrated a shift in BODIPY fluorescence toward red wavelengths in ML-IV (but not in normal) fibroblasts.

possibility that fluorescent lipid accumulation in the lysosomes of ML-IV cells was due to the general storage of various macromolecules in the lysosomes or to the enlarged volume of these organelles.

These studies demonstrate that C$_5$-DMB-LacCer accumulates in the lysosomes of ML-IV cells and show that its degradation is similar to that seen in normal cells. Similar results on the accumulation and degradation of radiolabeled lipids have been observed previously (3, 4). Thus, the accumulation of BODIPY-LacCer in the lysosomes of ML-IV cells is not due to an alteration in its degradation but rather to some other process. To examine the possibility that the ML-IV phenotype results from an alteration in membrane transport and/or recycling along the endocytic pathway, we carried out a detailed study of endocytosis in this cell type with a variety

Table 1. Hydrolysis of BODIPY-LacCer in normal *vs.* ML-IV fibroblasts

Incubation conditions	% hydrolysis	
	Normal	ML-IV
Pulse (1 hr; 19°C) → Chase (1 hr; 37°C)	7	6
Pulse (1 hr; 37°C) → Chase (1 hr; 37°C)	42	32
Pulse (1 hr; 37°C) → Chase (3 hr; 37°C)	74	68

Cells were incubated with C$_5$-DMB-LacCer/BSA for 1 hr at 19°C or 37°C, washed, and further incubated for 1 or 3 hr at 37°C before lipid extraction and analysis. Percent hydrolysis is [(C$_5$-DMB-metabolites)/ (C$_5$DMB-LacCer + C$_5$-DMG-metabolites)] × 100, where the C$_5$-DMB-metabolites were C$_5$-DMB-Cer, -GlcCer, and -SM. For a 1-hr pulse/1-hr chase (both at 37°C), the values in normal *vs.* ML-IV cells, respectively, were C$_5$-DMB-LacCer (58.2 ± 1.1% *vs.* 68.2 ± 0.4%), -Cer (16 ± 0.6% *vs.* 11.6 ± 0.2%), -GlcCer (12.3 ± 0.2% *vs.* 9.9 ± 0.1%), and -SM (13.3 ± 0.2% *vs.* 10.3 ± 0.1%). GlcCer, glucosylceramide; SM, sphingomyelin.

of markers to study different portions of the pathway diagrammed in Fig. 2.

Membrane Internalization and "Recycling." We first examined endocytosis of various markers at 19°C, a temperature at which internalization of components from the plasma membrane (or bathing medium) occurs but a temperature that inhibits transport beyond the "sorting endosome" compartment (26–29). No differences in the uptake of a fluid-phase marker (HRP), a marker for receptor-mediated endocytosis (^{125}I-Tfn), or a plasma membrane lipid marker (C$_5$-DMB-LacCer) were seen between normal and ML-IV fibroblasts (Table 2). Furthermore, no obvious differences in the number and distribution of endosomes was seen by fluorescence microscopy of the two cells types after a 60-min incubation at 19°C with C$_5$-DMB-LacCer (and back-exchange with defatted BSA; see Fig. 4, 0 min). Next, transport from the sorting endosomes to the plasma membrane ("recycling") was studied. Cells were incubated with ^{125}I-Tfn for 1 hr at 19°C, washed, "acid stripped" to remove any labeled Tfn from the cell surface, and then warmed to 37°C for various times. The amount of ^{125}I-Tfn present within the cells, at the cell surface, and released into the medium was determined (Fig. 3). Consistent with previous studies of membrane recycling in human skin fibroblasts (5, 30), recycling of ^{125}I-Tfn was very rapid.
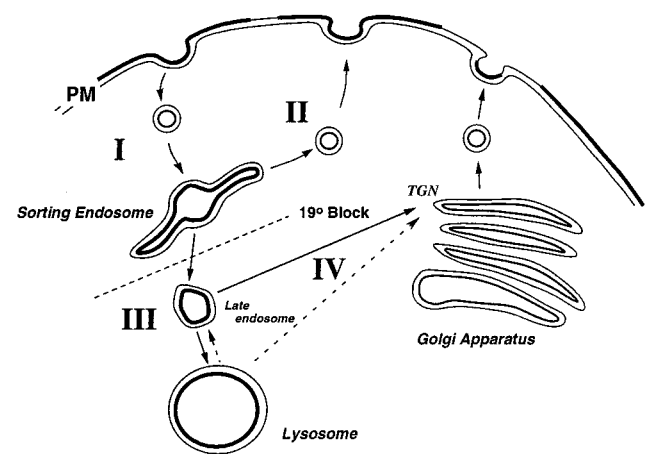

FIG. 2. Vesicular transport along the lysosomal pathway. Pathway I, transport from the plasma membrane (PM) to "sorting endosomes." The latter is experimentally defined by the use of a 19°C temperature block. Pathway II, "recycling" from sorting endosomes back to the plasma membrane. Pathway III, transport from sorting endosomes to lysosomes, was studied by measuring the concentration-dependent spectral changes in fluorescence as a BODIPY-lipid accumulated in the lysosomes. Pathway IV, alternative pathways for lipid transport to the Golgi complex. TGN, trans-Golgi network.

Table 2. Uptake of various markers into sorting endosomes

Marker	Normal	ML-IV
HRP, ng/μg of cell protein	0.70 $\pm$ 0.20	0.67 $\pm$ 0.10
C_5-DMB-LacCer, pmol/μg of DNA	6.10 $\pm$ 0.90	6.80 $\pm$ 0.20
^{125}I-Tfn,* cpm/μg of protein	0.974 $\pm$ 0.083	0.970 $\pm$ 0.042

Cells were incubated with the indicated marker for 1 hr at 19°C and washed. For C_5DMB-LacCer and ^{125}I-Tfn, cells were then back-exchanged or "acid stripped," respectively, to remove any marker from the plasma membrane before analysis.
*In a typical experiment, each sample contained at least, 1,000–1,500 cpm above background.

Furthermore, no differences in the recycling kinetics were seen between normal and ML-IV fibroblasts. Because previous studies using a fluorescent lipid analog demonstrated similar recycling kinetics of lipid and labeled Tfn (31, 32), we did not carry out additional recycling studies using labeled lipids. Thus, these data demonstrate that both the internalization and recycling pathways (Fig. 2, pathways I and II) are normal in ML-IV cells.

Transport from Sorting Endosomes to Lysosomes. We developed an assay to observe and quantify C_5-DMB-LacCer accumulation in the lysosomes (Fig. 2, pathway III). Cells were preincubated with blue dextran to label lysosomes and then incubated with C_5-DMB-LacCer for 60 min at 19°C (and back-exchanged) to label the sorting endosomes. The cells were then warmed for various times at 37°C to initiate transport to lysosomes. Images of the same cell were acquired at green and red wavelengths for the BODIPY-lipid and at blue wavelengths for the fluorescent dextran. Representative images at several times points are shown in Fig. 4. From 0 to 20 min (both cell types), the fluorescent lipid was present mostly in endosomes that were widely distributed throughout the cytoplasm and these endosomes did not coincide with the dextran-labeled lysosomes. At later times (20–60 min), colocalization of the BODIPY-lipid with a fraction of the lysosomes became increasingly apparent in ML-IV cells (see Fig. 4 *Inset*). Furthermore, large amounts of red fluorescence were
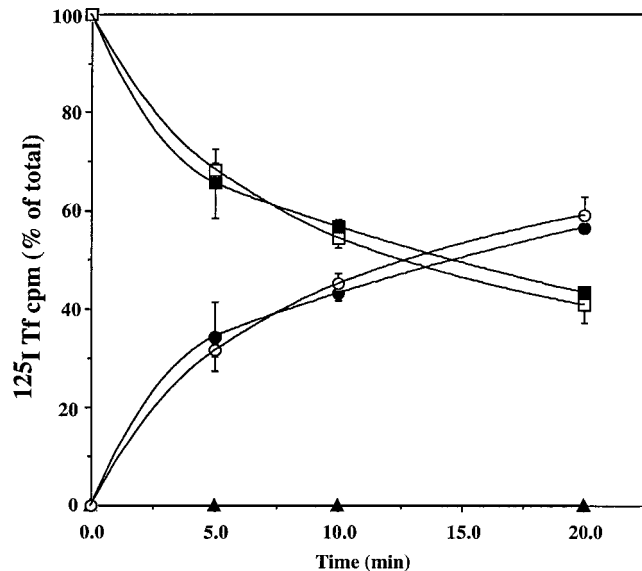

FIG. 3. Recycling kinetics in normal vs. ML-IV cells. Normal (●, ■, and ▲) and ML-IV (○, □, and △) fibroblasts were incubated with ^{125}I-Tfn for 60 min at 19°C, washed, and "acid-stripped" to remove any labeled Tfn at the plasma membrane. The cells were then warmed to 37°C for various times after which the amount of cell-associated ^{125}I-Tfn (surface, ▲ and △; intracellular, ■ and □) and ^{125}I-Tfn released into the medium (● and ○) was determined.

seen at these time points, indicating an accumulation of the BODIPY-lipid in this compartment. Some BODIPY-lipid could also be seen in the lysosomes of normal fibroblasts at 40 min; however, accumulation was less pronounced than in ML-IV cells. Finally, labeling of the Golgi apparatus was readily apparent in normal cells at 60 min, whereas little or no labeling of this organelle was seen in ML-IV fibroblasts at this time point.

Temporal changes in the accumulation of BODIPY-lipid at the lysosomes could be determined by measuring the change in the R/G ratio of the lysosomes with time at 37°C. After the 19°C incubation, quantitative studies showed that the R/G ratio of individual endosomes was nearly the same (0.287 $\pm$ 0.10 for normal vs. 0.247 $\pm$ 0.07 for ML-IV), indicating the concentration of C_5-DMB-LacCer in endosomes was similar in the two cell types. The cells were then warmed to 37°C for various times and the R/G ratio of the lysosomes was determined. (Because only a fraction of the endocytic vesicles at any given time corresponded to lysosomes, a "mask" based on the blue dextran image of each cell was used to identify those vesicles that would be used in the calculation of the R/G ratio.) As shown in Fig. 5, the lysosomal R/G ratio increased more rapidly in ML-IV cells than in normal fibroblasts between 0 and 40 min, suggesting that the apparent concentration of the BODIPY-lipid increased more rapidly in ML-IV cells relative to normal fibroblasts. After 40 min at 37°C, the R/G ratio of the lysosomes in ML-IV cells reached a plateau, whereas in normal cells the R/G ratio decreased, presumably reflecting a loss of BODIPY-lipid from the lysosomes.

Lipid Transport to the Golgi Complex. When cells were incubated with C_5-DMB-LacCer for 1 hr at 19°C, washed, back-exchanged, and further incubated for 1 hr at 37°C, labeling of the Golgi apparatus was readily seen in normal but not in ML-IV cells (see Fig. 4, 60 min). The pathway by which fluorescent lipid is transported beyond the "19°C block" to the Golgi complex (Fig. 2, pathway IV) is unknown. One possibility is that in normal cells, direct transport from the late endosomes to the Golgi complex occurs, but transport to the lysosomes is relatively minor. Consistent with this pathway are the observations that (*i*) a fraction of endocytosed Shiga toxin, a glycolipid-binding toxin, is transported to the trans-Golgi network (33–36) during internalization and (*ii*) some exogenous glycosphingolipid analogs are transported in part to the Golgi complex during endocytosis (37, 38). In this model, "lipid sorting" between the Golgi and the lysosomes would be altered in ML-IV cells, perhaps due to alteration of membrane properties or lysosomal accumulation of endogenous lipids. A second possibility is that some fluorescent lipid moves to the Golgi complex by a nonvesicular pathway. This would be consistent with the *in vitro* properties of BODIPY-Cer (spontaneous transbilayer movement and free diffusion between membranes; ref. 39) and with its high affinity for the Golgi apparatus (7, 23–25, 40). However, at the 60-min time point shown in Fig. 4, only 6–7% of the C_5-DMB-LacCer had been hydrolyzed in both cell types (Table 1), suggesting that the majority of Golgi fluorescence was due to C_5-DMB-LacCer, a lipid that does not exhibit spontaneous transbilayer movement *in vitro* (unpublished observations).

Analysis of Endogenous Ceramide. Endogenous lipids from normal and ML-IV cells were extracted and analyzed by several different methods. In each method, we found elevated levels of ceramide in ML-IV cells compared with normal fibroblasts. This elevation of ceramide could be quantified by using cells that were labeled to steady state with [1-^{14}C]palmitate and was found to be 5- to 12-fold higher than that seen in normal cells. Lysosomal accumulation of various sphingolipids and phospholipids has been extensively documented in ML-IV cells, and now we report increased ceramide levels in this cell type. Previous studies have shown that elevation of intracellular ceramide (achieved by incubating cells with exogenous
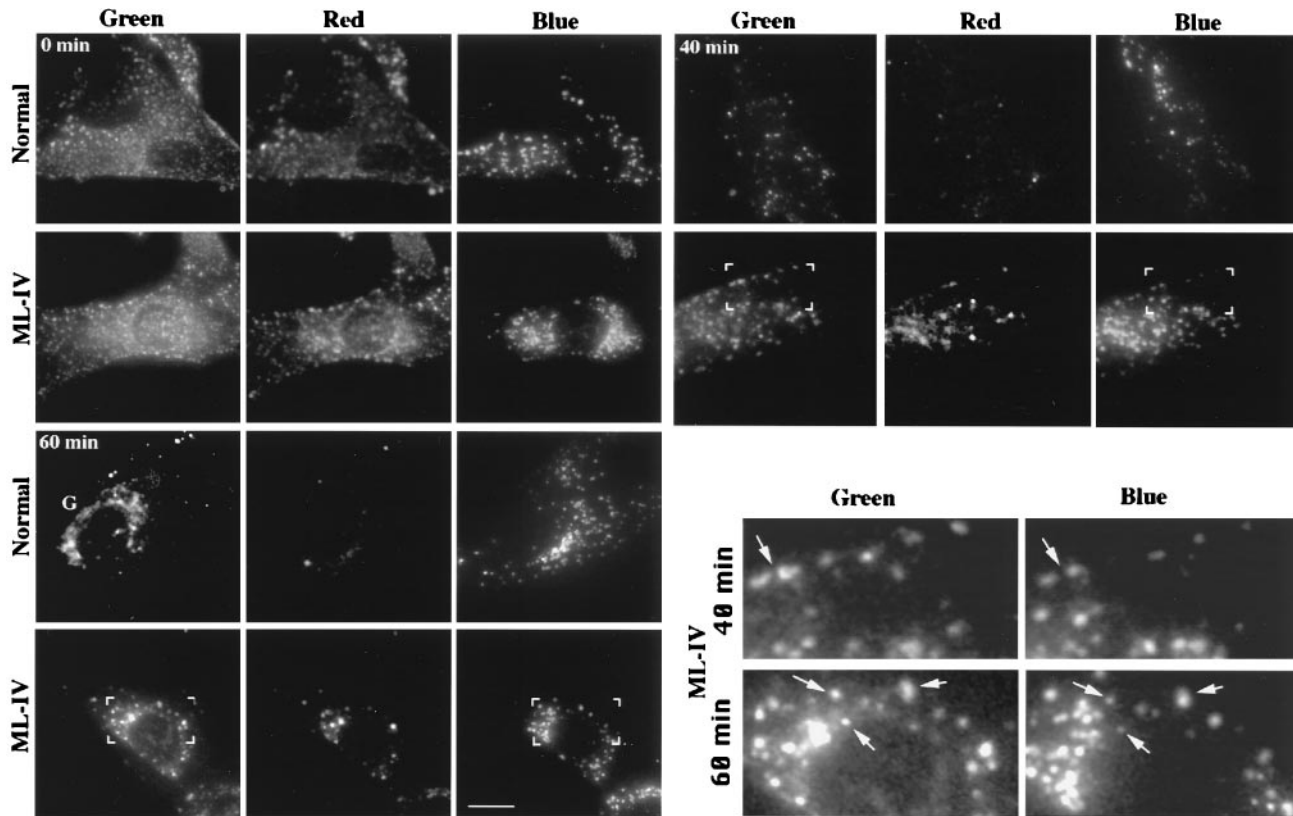
FIG. 4.   Transport of C$_5$-DMB-LacCer from sorting endosomes to lysosomes in normal vs. ML-IV cells. Normal or ML-IV cells were preincubated with blue dextran to label the lysosomes. The cells were then incubated for 1 hr at 19°C with 5 μM C$_5$-DMB-LacCer/defatted BSA, washed, back-exchanged with 5% defatted BSA, and further incubated for the indicated times at 37°C. Samples were photographed in the blue (dextran), green (BODIPY), and red (BODIPY) regions of the spectrum. (*Inset*) Bracketed regions show that some of the BODIPY-labeled vesicles are coincident with the lysosomes of ML-IV cells (e.g., at arrows). Also, note the labeling of the Golgi complex (G) in normal but not ML-IV fibroblasts at 60 min. (Bar = 10 μm.)

short-chain ceramide analogs or by treating cells with sphingomyelinase) can modulate transport along the secretory (41, 42) and endocytic (15) pathways. In the latter study, elevated levels of ceramide induced a redistribution of lysosomes to the perinuclear region of cells, reminiscent of the distribution of lysosomes in ML-IV cells that appeared to be larger than in normal cells and clustered about the nucleus (Figs. 1 and 4). Elevated ceramide levels also partially inhibit both fluid-phase and receptor-mediated endocytosis. Although this result seems inconsistent with the enhanced lysosomal accumulation of lipid found in the present study, the treatments described above are likely to elevate ceramide throughout the cell, whereas in ML-IV cells, increases in ceramide may be restricted to the lysosomes. If so, its presence there could exert a "local" effect on transport into and out of this organelle, as observed in our study. Further studies on the distribution of endogenous ceramide in ML-IV cells would help address this question. Experiments to determine whether decreasing intracellular ceramide (e.g., by use of inhibitors of ceramide synthesis) affects the ML-IV phenotype are also of great interest.

In summary, we have performed a detailed analysis of transport through the endocytic and lysosomal compartments of ML-IV cells and have shown that there is a defect in this cell type that affects late steps in the endocytic pathway. This is in contrast to the majority of endocytosis mutants described to date that are defective in earlier steps in this pathway. Our findings are consistent with the recent studies by Bargal and Bach (4) who showed that although the degradation of exogenously supplied radiolabeled lipids was normal in ML-IV cells, there was nevertheless accumulation in the lysosomes as assessed by subcellular fractionation studies. A defect in in

sorting and/or transport along the late endocytic pathway, rather than a defect in degradation might explain the absence
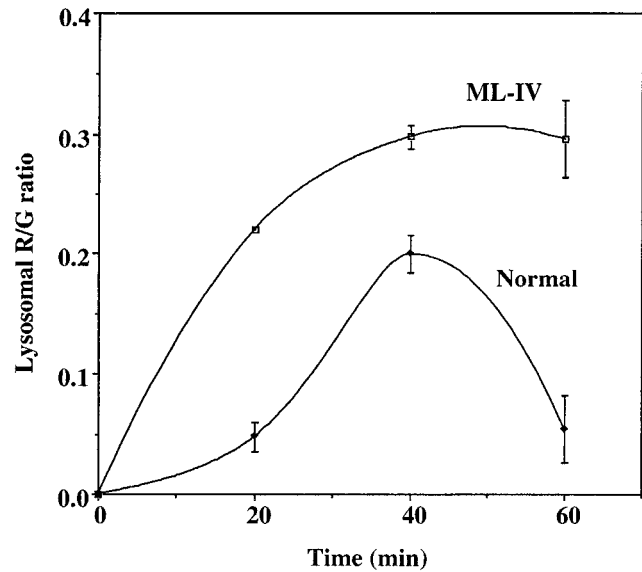

FIG. 5.   Temporal changes in accumulation of C$_5$-DMB-LacCer at the lysosomes. Normal and ML-IV cells were incubated with blue dextran and C$_5$-DMB-LacCer/defatted BSA as in Fig. 4. Images were acquired at each time point and the R/G ratio of individual lysosomes was quantified. Attempts to quantify the R/G ratio at earlier time points were not reliable because there was often substantial overlap of lysosomes and endosomes in the same region of the cell at these times, making it difficult to generate an appropriate "lysosome mask" for these calculations.

of massive buildup of materials as seen in other storage diseases. This, in turn, could explain some of the unique features of ML-IV such as (*i*) the lack of progression in clinical manifestations of the disease and the apparent "steady state" attained by these patients for at least two to three decades of life, (*ii*) the lack of organomegaly, despite the fact that lysosomal storage is seen in the liver and spleen, as well as other organs and tissues, and (*iii*) the unique spectrum of stored materials that is unlike that in most other lysosomal storage disorders.

1. Bach, G., Zeigler, M., Kohn, G. & Cohen, M. M. (1977) *Am. J. Hum. Genet.* **29,** 610–618.
2. Amir, N., Zlotogora, J. & Bach, G. (1987) *Pediatrics* **79,** 953–959.
3. Bach, G., Zeigler, M. & Bargal, R. (1998) in *Advances in Jewish Genetic Diseases*, ed. Desnick, R. J. (Oxford Univ. Press, New York), in press.
4. Bargal, R. & Bach, G. (1997) *J. Inherited Metab. Dis.* **20,** 625–631.
5. Koval, M. & Pagano, R. E. (1990) *J. Cell Biol.* **111,** 429–442.
6. Martin, O. C. & Pagano, R. E. (1994) *J. Cell Biol.* **125,** 769–781.
7. Pagano, R. E. & Martin, O. C. (1997) in *Cell Biology: A Laboratory Handbook*, ed. Celis, J. E. (Academic, New York), pp. 505–510.
8. Chen, C.-S., Martin, O. C. & Pagano, R. E. (1997) *Biophys. J.* **72,** 37–50.
9. Pagano, R. E., Martin, O. C., Kang, H. C. & Haugland, R. P. (1991) *J. Cell Biol.* **113,** 1267–1279.
10. Bligh, E. G. & Dyer, W. J. (1959) *Can. J. Biochem. Physiol.* **37,** 911–917.
11. Koval, M. & Pagano, R. E. (1989) *J. Cell Biol.* **108,** 2169–2181.
12. van Echten, G., Iber, H., Stotz, H., Takatsuki, A. & Sandhoff, K. (1990) *Eur. J. Cell Biol.* **51,** 135–139.
13. Krebs, K. G., Heusser, D. & Wimmer, H. (1969) in *Thin-Layer Chromatography*, ed. Stahl, E. (Springer, New York), Chap. Z.
14. Marsh, M., Schmid, S., Kern, H., Harm, E., Male, P., Mellman, I. & Helenius, A. (1987) *J. Cell Biol.* **104,** 875–886.
15. Chen, C.-S., Rosenwald, A. G. & Pagano, R. E. (1995) *J. Biol. Chem.* **270,** 13291–13297.
16. Lowry, O. H., Rosebrough, N. J., Farr, A. L. & Randall, R. J. (1951) *J. Biol. Chem.* **193,** 265–275.
17. Hunter, W. M. & Greenwood, F. C. (1962) *Nature (London)* **194,** 490–495.
18. Hopkins, C. R. & Trowbridge, I. S. (1983) *J. Cell Biol.* **97,** 508–521.
19. Labarca, C. & Paigen, K. (1980) *Anal. Biochem.* **102,** 344–352.
20. Goldin, E., Blanchette-Mackie, E. J., Dwyer, N. K., Pentchev, P. G. & Brady, R. O. (1995) *Pediatr. Res.* **37,** 687–692.
21. Bright, G. R., Fisher, G. W., Rogowska, J. & Taylor, D. L. (1987) *J. Cell Biol.* **104,** 1019–1033.
22. Pagano, R. E. & Chen, C.-S. (1998) *Ann. N. Y. Acad. Sci.,* **845,** 152–160.
23. Lipsky, N. G. & Pagano, R. E. (1985) *Science* **228,** 745–747.
24. Pagano, R. E. (1990) *Biochem. Soc. Trans.* **18,** 361–366.
25. Rosenwald, A. G. & Pagano, R. E. (1993) *Adv. Lipid Res.* **26,** 101–118.
26. Dunn, W. A., Hubbard, A. L. & Aronson, Jr., N. N. (1980) *J. Biol. Chem.* **255,** 5971–5978.
27. Aulinskas, T. H., Coetzee, G. A., Gevers, W. & van der Westhuyzen, D. R. (1982) *Biochem. Biophys. Res. Commun.* **107,** 1551–1558.
28. Helenius, A., Mellman, I., Wall, D. & Hubbard, A. (1983) *Trends Biochem. Sci.* **8,** 245–250.
29. Salzman, N. H. & Maxfield, F. R. (1989) *J. Cell Biol.* **109,** 2097–2104.
30. Goldstein, J. L., Brown, M. S., Anderson, R. G. W., Russell, D. W. & Schneider, W. J. (1985) *Annu. Rev. Cell Biol.* **1,** 1–39.
31. Koval, M. & Pagano, R. E. (1991) *Biochim. Biophys. Acta* **1082,** 113–125.
32. Mayor, S., Presley, J. F. & Maxfield, F. R. (1993) *J. Cell Biol.* **121,** 1257–1269.
33. Prydz, K., Hansen, S. H., Sandvig, K. & van Deurs, B. (1992) *J. Cell Biol.* **119,** 259–272.
34. Sandvig, K. Dubinina, E., Garred, Ø., Prydz, K., Kozlov, J. V., Hansen, S. H. & van Deurs, B. (1992a) *Biochem. Soc. Trans.* **20,** 724–727.
35. Sandvig, K., Garred, Ø., Prydz, K., Kozlov, J. V., Hansen, S. H. & van Deurs, B. (1992b) *Nature (London)* **358,** 510–511.
36. Garred, Ø., Dubinina, E., Holm, P. K., Olsnes, S., van Deurs, B., Kozlov, J. V. & Sandvig, K. (1995) *Exp. Cell Res.* **218,** 39–49.
37. Schwarzmann, G. & Sandhoff, K. (1990) *Biochemistry* **29,** 10865–10871.
38. Schwarzmann, G., Hofmann, P., Pütz, U. & Albrecht, B. (1995) *J. Biol. Chem.* **270,** 21271–21276.
39. Bai, J. & Pagano, R. E. (1997) *Biochemistry* **36,** 8840–8848.
40. Pagano, R. E., Sepanski, M. A. & Martin, O. C. (1989) *J. Cell Biol.* **109,** 2067–2079.
41. Rosenwald, A. G. & Pagano, R. E. (1993) *J. Biol. Chem.* **268,** 4577–4579.
42. Linardic, C. M., Jayadev, S. & Hannun, Y. A. (1996) *Cell Growth Differ.* **7,** 765–774.